

## Adsorption of Ionic Surfactants to a Plasma Polymer Substrate

R. Atkin,<sup>†,‡</sup> V. S. J. Craig,<sup>§</sup> P. G. Hartley,<sup>||</sup> E. J. Wanless,<sup>\*,†</sup> and S. Biggs<sup>†,⊥</sup>

*Discipline of Chemistry, School of Environmental and Life Sciences, The University of Newcastle, Callaghan, NSW 2308, Australia; Department of Applied Mathematics, Research School of Physical Sciences & Engineering, Australian National University, Canberra ACT 0200, Australia; and CSIRO Molecular Science, Bag 10, Clayton South, Victoria 3169, Australia*

Received November 14, 2002. In Final Form: February 25, 2003

The adsorption of an anionic C<sub>12</sub> surfactant and cationic C<sub>12</sub> and C<sub>16</sub> surfactants to a synthetic, anionic radio frequency glow discharge plasma polymer substrate has been investigated. This substrate has a similar charge density to that of amorphous silica but also possesses hydrophobic character, producing a water sessile contact angle of about 74° at pH values between 2 and 7. Both the cationic and anionic C<sub>12</sub> surfactants had the same saturation surface excess values on the plasma polymer substrate. Surprisingly, the addition of electrolyte did not affect the saturation surface excess, indicating that hydrophobic interactions between the surfactants and the substrate dominate the adsorption process. All surfactant systems show a change in slope in the isotherm at a surface excess of 0.3 mg·m<sup>-2</sup>. The likely conformation of the adsorbed surfactants at this surface excess is with the monomer lying flat on the substrate, to maximize hydrophobic interactions between the hydrocarbon chain and the surface. As the bulk concentration is increased further, adsorption is dominated by hydrophobic interactions. The structure of the adsorbed layer at saturation is discussed.

### Introduction

Surfactants at solid–liquid interfaces are known to self-assemble into structured aggregates.<sup>1–5</sup> Recently, it has been demonstrated that the aggregate structure<sup>6,7</sup> can profoundly influence the surfactant adsorption density<sup>8</sup> and the adsorption kinetics.<sup>9,10</sup> Therefore, the performance of surfactants either in flotation, as detergents, or as wetting agents will be influenced by the surfactant aggregates that form at the solid–liquid interface. These structures result from a balance of the interactions between surfactant monomers with the interactions between monomers and the substrate and from geometrical packing constraints. Aggregate structures have been elucidated on hydrophilic crystalline surfaces, hydrophobic crystalline surfaces, and hydrophilic amorphous surfaces. Here

we present a study of ionic surfactant adsorption onto a moderately hydrophobic amorphous polymer surface and deduce the morphology of the aggregates that are formed.

Grant et al.<sup>11</sup> have previously investigated nonionic surfactant aggregation at an amorphous hydrophobic surface, prepared by covalently attaching diethyloctylchlorosilane (DEOS) to a silica substrate. A uniform monolayer formed at the surface, with headgroups facing into solution and the surfactant hydrocarbon chains interacting hydrophobically with the hydrocarbon chain of DEOS. Wolgemuth et al.<sup>12</sup> have studied the adsorption of various surfactants to an amorphous silica surface, hydrophobized by the covalent attachment of trimethylchlorosilane (TMCS). It was found that the interfacial aggregates formed were roughly hemispherical, in contrast to the hemicylindrical structures formed on crystalline hydrophobic substrates. The surfactant morphology observed was independent of the type of headgroup, leading the authors to suggest that adsorption was driven by hydrophobic interactions between the substrate and surfactant hydrocarbon chains. Notably, SDS adsorption was not observed on the TMCS substrate. This was attributed to electrostatic repulsion between the surfactant monomers and a small residual negative charge on the silica, after reaction with TMCS. This observation is of importance to the current investigation. Grant et al.<sup>13</sup> systematically investigated the influence of substrate hydrophobicity on the adsorption of a nonionic surfactant. The substrate hydrophobicity was varied by manipulation of the hydroxy/methyl ratio of the terminal groups of surface bound long chain thiols. It was shown that as the interface was rendered progressively more hydrophobic, the structure at the substrate changed from diffuse

\* Corresponding author. Telephone: +61 2 4921 8846. Facsimile: +61 2 4921 5472. E-mail: ewanless@mail.newcastle.edu.au.

<sup>†</sup> The University of Newcastle.

<sup>‡</sup> Current address: School of Chemistry, University of Bristol, Cantock's Close, Bristol BS8 1TS, United Kingdom. E-mail: Rob.Atkin@Bristol.ac.uk.

<sup>§</sup> Australian National University. E-mail: vince.craig@anu.edu.au.

<sup>||</sup> CSIRO Molecular Science. E-mail: Patrick.Hartley@csiro.au.

<sup>⊥</sup> Current address: School of Process, Environmental and Materials Engineering, University of Leeds, Leeds LS2 9JT, United Kingdom. E-mail: s.r.biggs@leeds.ac.uk.

(1) Fuerstenau, D. W.; Wakamatsu, T. *Faraday Discuss. Chem. Soc.* **1975**, *59*, 157.

(2) Somasundaran, P.; Fuerstenau, D. W. *J. Phys. Chem.* **1966**, *70*, 90.

(3) Gao, Y.; Du, J.; Gu, T. *J. Chem. Soc., Faraday Trans. 1* **1987**, *83*, 2671.

(4) Gaudin, A. M.; Fuerstenau, D. W. *Trans. AIME* **1955**, *202*, 958.

(5) Yeskie, M. A.; Harwell, J. H. *J. Phys. Chem.* **1988**, *92*, 2346.

(6) Manne, S.; Gaub, H. E. *Science* **1995**, *270*, 1480.

(7) Manne, S.; Schaffer, T. E.; Huo, Q.; Hansma, P. K.; Morse, D. E.; Stucky, G. D.; Aksay, I. A. *Langmuir* **1997**, *13*, 6382.

(8) Velegol, S. B.; Fleming, B. D.; Biggs, S.; Wanless, E. J.; Tilton, R. D. *Langmuir* **2000**, *16*, 2548.

(9) Atkin, R.; Craig, V. S. J.; Biggs, S. *Langmuir* **2001**, *17*, 6155.

(10) Atkin, R.; Craig, V. S. J.; Wanless, E. J.; Biggs, S. *Adv. Colloid Interface Sci.*, in press.

(11) Grant, L. M.; Tiberg, F.; Ducker, W. A. *J. Phys. Chem. B* **1998**, *102*, 4288.

(12) Wolgemuth, J. L.; Workman, R. K.; Manne, S. *Langmuir* **2000**, *16*, 3077.

(13) Grant, L. M.; Ederth, T.; Tiberg, F. *Langmuir* **2000**, *16*, 2291.

micellar coverage, to dense micellar coverage, to bilayer coverage, to monolayer coverage on the most hydrophobic surface.

These results indicate that as the level of substrate hydrophobicity increases, it is the hydrophobic interactions between the substrate and the surfactant that dominate the adsorption process. This is in contrast to the results obtained on less hydrophobic mineral oxide surfaces such as silica<sup>14</sup> and alumina.<sup>15</sup> In these cases, increases in adsorption above that required for surface charge neutralization are due to the formation of an admicelle via the hydrophobic interactions that occur between the hydrocarbon chains of adsorbing surfactants and those electrostatically bound to the surface.

While the interactions between surfactants and a solid polymeric interface have not been investigated in detail, the analogous interactions between polymers and surfactants *in solution* have been extensively studied due to their importance to many industrial processes.<sup>16–19</sup> Adsorption of an ionic surfactant to a nonionic polymer begins at the critical aggregation concentration (cac), which is below the cmc and is dependent on both the surfactant type and the polymer hydrophobicity. The association of an ionic surfactant to an oppositely charged polyelectrolyte typically occurs readily, even at low bulk surfactant concentrations, due to electrostatic attraction. In this case, the cac may be several orders of magnitude lower than the solution surfactant cmc.<sup>20,21</sup> Conversely, the interactions between an ionic surfactant and a polymer of like charge will not readily occur, as an electrostatic barrier to association must be overcome.<sup>22</sup> However, it has been shown that binding may occur if the polyelectrolyte is rendered sufficiently hydrophobic, so that attraction between the hydrocarbon chains of the surfactant and the polymer chain is sufficient to overcome the Coulombic repulsions.<sup>23,24</sup> Analogous behavior is anticipated on a solid polymeric substrate.

In this study we use optical reflectometry and atomic force microscopy to investigate the adsorption of cetyltrimethylammonium bromide (CTAB), dodecyltrimethylammonium bromide (DTAB), and sodium dodecyl sulfate (SDS) to an amorphous, negatively charged, hydrophobic surface created by plasma polymerization on an oxidized silicon wafer substrate.<sup>25</sup> Applying a thick polymer film to a bulk material is an effective means of modifying its interfacial properties. These films are being developed as coatings for the purpose of increasing bonding efficiency between surfaces, as biocompatible surfaces,<sup>26</sup> and to protect a material from chemical or physical attack. Plasma polymerization may facilitate attachment of a

specific chemical functional group or the modification of surface properties, such as wetting.

## Materials and Methods

The acetaldehyde plasma polymer (AAPP) coated silicon wafers were obtained from CSIRO Molecular Science, Melbourne, Australia. The method of preparation is described extensively elsewhere.<sup>25</sup> Briefly, silicon wafers with an oxide thickness of 30 nm are placed in a custom built reactor. The cylindrical reactor chamber has a diameter of 17 cm and is 35 cm high. Samples were placed on the lower, circular electrode (of diameter 9.5 cm) while the upper electrode was U-shaped. The distance between the electrodes was 12.5 cm. Acetaldehyde plasma depositions were achieved using a frequency of 125 kHz, a power of 10 W, and an initial acetaldehyde monomer pressure of 40 Pa for four periods of 1 min, resulting in a polymer film 110 nm thick. The thickness of the polymer layer is critical for the calculation of the sensitivity factor used in optical reflectometry, and was determined using masking and AFM imaging. The method is described in detail elsewhere.<sup>26</sup>

The AAPP surface had a water sessile contact angle of 74°<sup>27</sup> and a  $\zeta$  potential of -70 mV in 1 mM electrolyte at pH 6.4,<sup>28</sup> which equates to approximately one negative charge per 5 nm<sup>2</sup>. The rms roughness of the AAPP surface was 4.4 nm.<sup>25</sup> This value is only slightly higher than that determined for the underlying silica substrate (3.7 nm) and should not affect the accuracy of the method. The refractive index used for the calculation of surface excess values for the AAPP film is 1.46. This is in the range 1.4–1.55, which has been reported previously for plasma polymer films.<sup>29,30</sup> Conveniently, it equals the refractive index of silica, allowing the silica and plasma polymer layer to be treated as one layer of thickness 140 nm in the Fresnel optical model used to calibrate the reflectometer sensitivity.<sup>31</sup>

The optical reflectometry technique is described by Dijt et al.<sup>32</sup> and has been discussed in detail previously.<sup>33</sup> Reflectometry relies upon the change in the reflective properties of a substrate upon adsorption of material. In a typical reflectometry experiment, the cell initially contains only water. Surfactant is then passed into the cell, and the change in the ratio of the p and s polarizations of the laser beam is recorded. This change is proportional to the surface excess. The proportionality constant is calculated using a four-layer Fresnel model of the interface. The reflectometer is contained within an incubator, allowing the temperature to be accurately maintained at 25.0 ± 0.1 °C.

CTAB and DTAB (purity greater than 99%) were obtained from Aldrich and twice recrystallized from acetone and freeze-dried prior to use. SDS (purity greater than 99%) and sodium bromide (purity greater than 99%) were obtained from Aldrich and used without further purification. All water used was filtered, distilled, and passed through a Millipore filtration unit before use.

## Results and Discussion

The reflectometer enables both the kinetics of adsorption and equilibrium surfactant surface excess values to be measured. To determine the equilibrium surface excess, the adsorption process was permitted to reach completion. This was indicated by a gradual decrease in the rate of adsorption with time until no further adsorption could be detected. Five surfactant systems were investigated. CTAB, DTAB, and SDS with no added electrolyte and DTAB and SDS in the presence of 10 mM sodium bromide. Numerous adsorption studies were performed. For clarity,

(14) (a) Goloub, T. P.; Koopal, L. K.; Bijsterbosch, B. H.; Sidorova, M. P. *Langmuir* **1996**, *12*, 3188. (b) Goloub, T. P.; Koopal, L. K. *Langmuir* **1997**, *13*, 673.

(15) Bohmer, M. R.; Koopal, L. K. *Langmuir* **1992**, *8*, 2649.

(16) Desai, N. N.; Shah, D. O. *Polym. Prepr.* **1981**, *22*, 39.

(17) Goddard, E. D. *J. Soc. Cosmet. Chem.* **1990**, *41*, 23.

(18) Allii, D.; Bolton, S.; Gaylord, N. S. *J. Appl. Polym. Sci.* **1991**, *42*, 947.

(19) Longer, M. A.; Ch'ng, H. S.; Roninson, J. R. *J. Pharm. Sci.* **1985**, *74*, 406.

(20) Thalberg, K.; Lindman, B.; Karlström, G. *J. Phys. Chem.* **1990**, *94*, 4289.

(21) Thalberg, K.; Lindman, B.; Karlström, G. *J. Phys. Chem.* **1991**, *95*, 3370.

(22) Binana-Limbele, M.; Zana, R. *Colloids Surf.* **1986**, *21*, 483.

(23) Anthony, O.; Zana, R. *Langmuir* **1996**, *12*, 1967.

(24) Benraou, M.; Zana, R.; Varoqui, R.; Pefferkorn, E. *J. Phys. Chem.* **1992**, *96*, 1468.

(25) Hartley, P. G.; Thissen, H.; Vaithianathan, T.; Griesser, H. J. *Plasma Polym.* **2000**, *5*, 47.

(26) Griesser, H. J.; et al. In *Plasma Deposition and Treatment of Polymers*; Lee, W. W., et al., Eds.; Materials Research Society: Warrendale, PA, 1999.

(27) Beumer, G. Unpublished data.

(28) Hartley, P. G.; McArthur, S.; McLean, K.; Griesser, H. J. *Langmuir* **2002**, *18*, 2483.

(29) Lassen, B.; Malmsten, J. *J. Colloid Interface Sci.* **1996**, *180*, 339.

(30) Vaithianathan, T. Ph.D. Thesis, University of New South Wales, 1999.

(31) Hansen, W. N. *J. Opt. Soc. Am.* **1968**, *58*, 380.

(32) Dijt, J. C.; Cohen Stuart, M. A.; Fleer, G. J. *Adv. Colloid Interface Sci.* **1994**, *50*, 79.

(33) Atkin, R.; Craig, V. S. J.; Biggs, S. *Langmuir* **2000**, *16*, 9374.

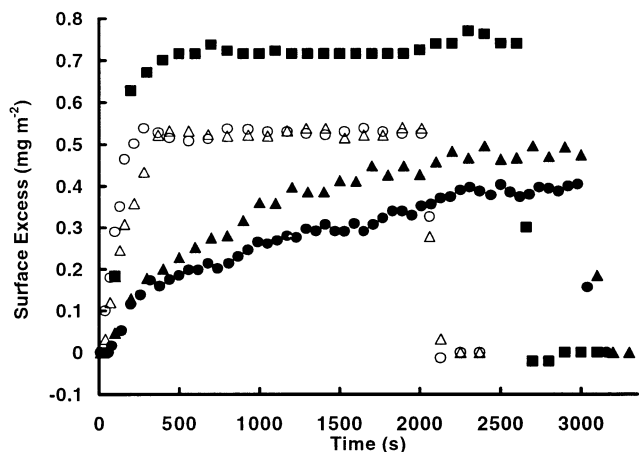


**Figure 1.** Representative adsorption experiments on the AAPP substrate for the five surfactant systems studied: 3.4 mM CTAB (■); 7.0 mM DTAB in no added electrolyte (▲); 7.1 mM DTAB in 10 mM NaBr (△); 8.4 mM SDS in no added electrolyte (●); 5.5 mM SDS in 10 mM NaBr (○). The concentrations presented all result in saturation levels of coverage for the corresponding adsorbed surfactant layer. Reductions in surface excess between 2000 and 3000 s correspond to desorption of surfactant upon water being passed into the cell.

only five adsorption results are presented in Figure 1. For each system, these results are representative of the adsorption process at concentrations where the maximum surface excess was reached.

**Adsorption Isotherms.** By performing numerous adsorption experiments at a range of concentrations, the adsorption isotherm can be determined for each system. The adsorption isotherms for the cationic surfactant systems, CTAB and DTAB (with and without added 10 mM NaBr), are presented in Figure 2A. The isotherms for the anionic surfactant system, SDS (with and without added 10 mM NaBr), are given in Figure 2B. The isotherms can be divided into four regions. Region 1 is a low surface excess region where the level of adsorption is independent of the bulk concentration. Regions 2 and 3 are where the surface excess is increasing linearly with concentration, the latter increasing more steeply, and region 4 is a final plateau region where no further adsorption is observed as the bulk concentration of surfactant is increased. We note that the first region is absent for the anionic surfactant systems shown in Figure 2B. This difference is clearly attributable to the negative surface charge on the AAPP substrate, which drives electrostatic adsorption of cationic surfactant and hinders adsorption of anionic surfactant.

In Figure 2A it can be seen that, up to a surfactant concentration of about 0.02 mM, the adsorption isotherms of CTAB and DTAB are indistinguishable. This indicates that the adsorption in the first region is independent of the hydrophobicity of the surfactant monomer and is thus driven purely by Coulombic attractions between the surfactants and the charged sites on the surface. In the DTAB + 10 mM NaBr system, the surface excess is much lower in this region of the isotherm. We attribute this difference to screening of the surfactant–surface electrostatic interaction and/or reduction in the number of charged sites suitable for adsorption on the surface due to adsorption of Na<sup>+</sup> ions. Similar effects have been observed on silica for the adsorption of CPBr.<sup>9</sup>

**Surface cac.** For all isotherms, further adsorption beyond region 1 takes place against a repulsive electrostatic interaction and therefore must be driven by

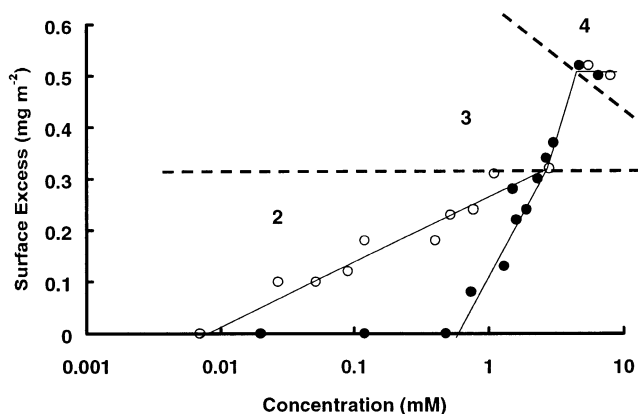
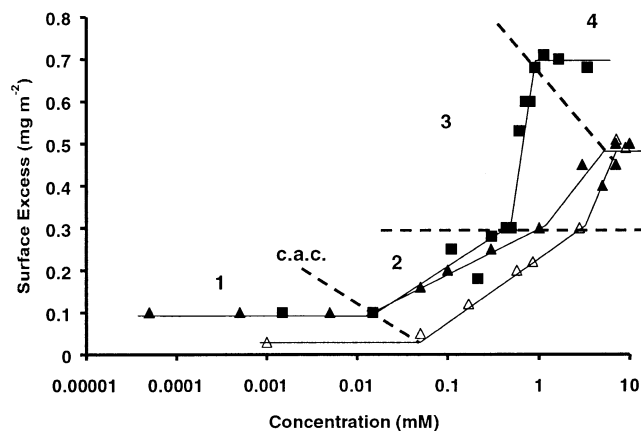


**Figure 2.** Adsorption isotherms on the AAPP substrate. The filled lines are drawn to guide the eye with regard to trends in the data series. The dashed lines separate the numbered regions of the isotherms. (A) The cationic systems: CTAB (■); DTAB in no added electrolyte (▲); DTAB in 10 mM NaBr (△). Within instrumental limitations, the adsorption isotherms for CTAB and DTAB with no added electrolyte are indistinguishable below 0.02 mM, as are the DTAB with no added electrolyte and DTAB with 10 mM NaBr isotherms above approximately 3 mM. (B) The anionic systems: SDS in no added electrolyte (●) and in 10 mM NaBr (○). Note that region 1 is not present. Within experimental limitations, the isotherms are indistinguishable above 3 mM.

hydrophobic interactions. The concentration which separates the first and second regions of the isotherm is analogous to the *cac* for surfactant–polymer interactions in solution,<sup>20</sup> and we shall call it the *surface cac*. For the cationic systems, the surface *cac* is determined by the hydrophobicity of both the substrate and the surfactant monomer. In the SDS systems the adsorption takes place against an additional electrostatic repulsion between the monomer headgroup and charged sites on the surface.

The surface *cac* for DTAB occurs at a higher surfactant concentration when 10 mM NaBr is present. This is in contrast to the behavior observed on mineral substrates.<sup>33</sup> Even after the surface *cac* is exceeded, the surface excess is less in the presence of 10 mM NaBr up to saturation levels of coverage. Again, for silica systems the opposite effect is observed.<sup>33</sup> We attribute this behavior to a considerable difference in the hydrophobicity of the systems with and without electrolyte. In the absence of electrolyte the surface charge is neutralized by surfactant monomers, thereby increasing the hydrophobicity of the surface. In the presence of electrolyte, much of the charge neutralization is due to adsorbed Na<sup>+</sup> ions, which will be hydrated. This effectively increases the hydrophilicity of

the surface. Clearly, hydrophobically driven adsorption will be more favorable in the absence of electrolyte. The important difference is that for this polymeric surface the adsorbed monomers are lying flat on the surface and further adsorption is taking place directly on the surface, whereas for mineral surfaces the adsorption is taking place primarily onto other monomers and not directly onto the surface.<sup>6-9</sup>

The opposite trend is observed in the SDS system. Here the addition of 10 mM NaBr results in a greatly reduced surface cac. This is attributable to the reduced electrostatic repulsions between the monomer and the surface upon addition of electrolyte. Surprisingly, the surface cac in the presence of electrolyte occurs at a lower concentration for SDS than it does for DTAB, despite the negative surface charge. This is due to the greater tendency of SDS to associate, which is evidenced by a lower cmc (8 mM as opposed to 14.5 mM for DTAB). Additionally, the influence of the unfavorable electrostatic interactions is dramatically reduced by the presence of electrolyte.

**Adsorption above the Surface cac.** In region two, all systems exhibit a logarithmic increase of surface excess with concentration above the surface cac. The slope of the isotherm in this region is indicative of the magnitude of the favorable hydrophobic surface-monomer interactions. The slope of the CTAB isotherm exceeds that of the DTAB isotherm. This is a direct consequence of the greater hydrophobicity of the C<sub>16</sub> versus C<sub>12</sub> hydrocarbon chain. Importantly, all the systems remain linear until the same surface excess of  $\sim 0.3 \text{ mg}\cdot\text{m}^{-2}$  is reached. Saturation of this adsorption process occurs at this concentration and strongly suggests that the arrangement of surfactants on the surface is the same in all systems. It is postulated that coverage of the substrate in this region is by random sequential adsorption. Adsorbed surfactant chains are confined to the plane of the substrate by hydrophobic interactions while the headgroups may protrude from the surface in order to maximize hydration. Calculation reveals that at the completion of region 2 a single layer of molecules lying prostrate on the substrate would occupy  $\sim 75\%$  of the surface area. As the substrate has no crystalline order to template surfactant ordering, this surface coverage may be the maximum obtainable when the surfactant chains are confined to the surface. Additionally, the presence of randomly positioned surface charges will serve to disrupt any ordering within the prostrate monolayer.

For the cationic surfactants, the surfactants adsorb opposite a surface charge, oriented with headgroups electrostatically bound to the charged surface group, and hydrocarbon chains adsorbed to the substrate. Between the charged substrate groups, surfactants are adsorbed with hydrocarbon chains against the hydrophobic surface, while the headgroups may be oriented toward the solution, depicted schematically in Figure 3A (side view). For SDS, it is anticipated that the surfactant will be adsorbed in the same manner as that for DTAB and CTAB but lie between charged surface sites. At the charged surface sites, sodium ions will adsorb. The likely conformation of the adsorbed SDS is presented in Figure 3B.

At the end of the second region, the SDS isotherms with and without added salt meet. Initially, the levels of adsorption in the presence of salt are far greater, but the surface excess increases more gradually. In comparison, the DTAB systems with and without salt differ in surface excess throughout this region.

**Third Region.** The next subregion occurs for surface excess values from  $0.3 \text{ mg}\cdot\text{m}^{-2}$  up to the saturation level of coverage for each system ( $\sim 0.5 \text{ mg}\cdot\text{m}^{-2}$  for C<sub>12</sub> systems

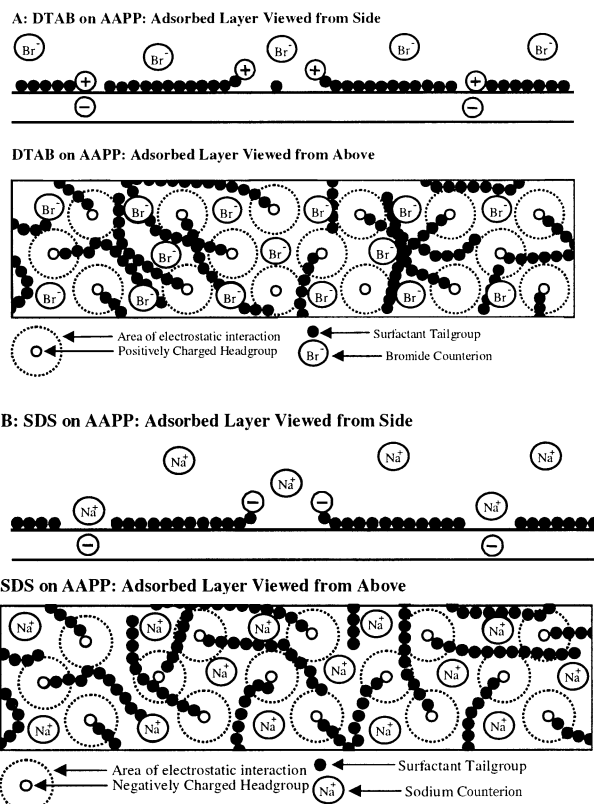


**Figure 3.** Schematic representation of the proposed prostrate monolayer conformation for the surfactants on the AAPP substrate: (A) cationic surfactant; (B) anionic surfactant. Added electrolyte is not expected to significantly alter this morphology. These diagrams are not drawn to scale.

and  $0.7 \text{ mg}\cdot\text{m}^{-2}$  for CTAB). The surface excess is now too large for all the surfactant monomers to be confined to a prostrate layer against the substrate. A more complex structure must exist. Throughout this region the level of SDS surface excess is unaffected by the presence of electrolyte. This indicates that electrostatic interactions have no influence on the adsorption of SDS in this region, suggesting that the concentration of adsorbed Na<sup>+</sup> ions has reached a maximum in region 2 and the SDS headgroup interactions are negligible. In comparison, the DTAB isotherms differ up until the surface excess has reached a maximum, indicating that, up to surface saturation levels, electrostatic interactions are influential.

This region of the isotherm exhibits the greatest rate of increase in surface excess with increasing bulk concentration. This rapid increase is a consequence of cooperative hydrophobic interactions between adsorbed and adsorbing monomers. The end result of this process is the plateau region of the adsorption isotherm, and further increases in concentration have no effect on surface excess.

**Plateau Adsorption.** The CTAB isotherm reaches a saturation surface excess of  $0.7 \text{ mg}\cdot\text{m}^{-2}$ . This is considerably less than the adsorption levels achieved on silica ( $1.6 \text{ mg}\cdot\text{m}^{-2}$ ),<sup>8,9</sup> where bilayered aggregates are known to form. The surface excess for the SDS and DTAB systems is even lower; therefore, we eliminate bilayered aggregates as possible surface aggregate structures. Perhaps then the surface morphology is similar to that on a strongly hydrophobic surface? Several AFM investigations have reported that graphite exerts a high degree of control over the aggregate structure due to a large interaction area

with the adsorbed surfactant.<sup>6,34</sup> Aggregation results from hydrophobic interactions between the exposed hydrocarbon chains of adsorbed surfactants and the hydrocarbon chains of surfactants in the bulk, producing the observed hemicylindrical aggregates. The recent calorimetric study of Kiraly and Findenegg supported this aggregate structure<sup>35</sup> and, most importantly for this investigation, reported a saturation surface excess of  $0.8 \text{ mg}\cdot\text{m}^{-2}$  for DTAB adsorption to graphite in the absence of electrolyte at  $25^\circ\text{C}$ . This value is 40% higher than the saturation surface excess obtained for all the  $\text{C}_{12}$  surfactant systems investigated in this study. Additionally, AFM images of surfactant surface aggregates on graphite substrates are readily obtained, while imaging of the AAPP surface was unable to reveal any structure in the adsorbed layer. Importantly, force versus distance data exhibited no evidence of a jump to contact in the force curves, supporting the finding that the adsorbed surfactant is strongly adsorbed and lying relatively flat on the substrate. We therefore conclude that tightly packed hemicylindrical aggregates are not present on the AAPP substrate.

Therefore, the structure of the surfactant layer on the AAPP substrate must be less ordered than the hemimicelles present on graphite. The  $\text{C}_{12}$  systems all show the same plateau level of surface excess, indicating that the level of electrolyte and the charge on the surfactant headgroup do not influence the final adsorbed structure at saturation levels of coverage. Hydrophobic interactions must be dominating. Further, the level of adsorption beyond the prostrate monolayer coverage achieved at the end of region 2 is not large ( $\sim 40\%$  of the total). The proposed structure is one of monomers adsorbed to the most hydrophobic patches of the prostrate monolayer. This will leave the more hydrophilic charged sites exposed to water. Thus, the overall structure is one of a prostrate monolayer with a partially ( $\sim 65\%$ ) complete second prostrate monolayer attached to it. The sparseness of the "second" layer ensures that headgroup interactions are not important. Note the "second" layer should not be considered a distinct layer, as it will be anchored in the prostrate layer and very incomplete. The lack of any order in the adsorbed layer results in laterally homogeneous AFM images.

For CTAB, the level of surface excess beyond the prostrate monolayer coverage is significant and contributes  $\sim 60\%$  of the total surface excess. The structure in this case may be similar to that of the hemimicelles present on graphite, but with a lower packing density and the disruption in packing due to charged surface sites, the layer will be very disordered. This will ensure that AFM images cannot reveal structural details.

The data obtained in this investigation do not discount the possibility of different surface morphologies (and higher surface excess values), at higher surfactant or salt concentrations; however, as the concentrations studied substantially exceed the solution cmc values, no increase in adsorption is expected at higher surfactant concentrations.

**Adsorption Kinetics.** For experiments designed to investigate the kinetics of initial adsorption, surfactant solutions were in contact with the surface for approximately 30 s before water was passed into the cell. This resulted in desorption of surfactant from the surface to levels below the detection limit of the instrumentation.

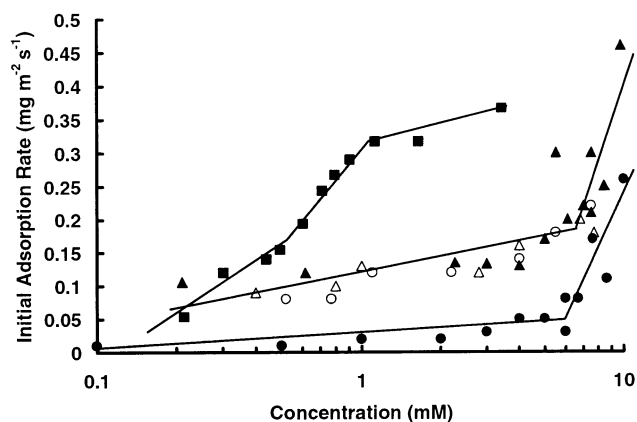


**Figure 4.** Initial adsorption rates on the AAPP substrate for CTAB (■), DTAB in no added electrolyte (▲) and in 10 mM NaBr (△), and SDS in no added electrolyte (●) and in 10 mM NaBr (○).

This cycle was completed 5 to 10 times in order to allow an average initial adsorption rate to be calculated.

The initial adsorption rates obtained for the five surfactant systems investigated on the AAPP surface are presented in Figure 4. In the first region of the isotherm, the observed surface excess values and the calculated rates of adsorption are low and the errors in the rate measurements substantial. Consequently, these values are not reported. As SDS does not adsorb to the AAPP surface appreciably until the solution surfactant concentration is approximately 1 mM, the rate of SDS adsorption between 0 and 1 mM is approximately zero. The rate of adsorption for CTAB is significantly higher than that of the  $\text{C}_{12}$  surfactants at all concentrations. This is due to the longer hydrocarbon chain of CTAB providing a greater hydrophobic driving force for adsorption.

The adsorption rates for DTAB and SDS with electrolyte and DTAB without added electrolyte are very similar throughout the concentration range. In contrast, the initial rate of adsorption for SDS without added electrolyte is lower than that obtained for all other surfactants. This directly reflects the electrostatic repulsion between SDS and the charged substrate.

For the five surfactant systems studied here, the adsorption rate increases as the cmc is approached (or exceeded for CTAB and the systems with added electrolyte). When similar results have been observed for cationic surfactants adsorbing to silica, analysis has revealed that micelles are adsorbed directly to the substrate.<sup>9,33</sup> This is possible because the types of aggregates formed on the silica surface and in solution have structural similarities. However, given the adsorbed layer morphology on the AAPP substrate, it is difficult to envisage direct adsorption of micelles to the substrate. Therefore, for the AAPP substrate, the increase in the rate of adsorption above the cmc is attributed to transport of monomers within micelles to the interface, whereby the transport within a micelle to the surface must be more effective than as a monomer.

## Conclusions

The adsorption of the cationic surfactants DTAB and CTAB, which are hydrophobically and electrostatically attracted to the AAPP substrate, has been observed. At a surface excess of  $\sim 0.3 \text{ mg}\cdot\text{m}^{-2}$ , all surfactant systems exhibit a change in the slope of the adsorption isotherm. At this level of surface excess, a prostrate monolayer with little order is present on the substrate.  $\text{C}_{12}$  surfactant systems, both anionic and cationic, with and without

(34) Manne, S.; Warr, G. G. In *Supramolecular Structure in Confined Geometries*; Manne, S., Warr, G. G., Eds.; American Chemical Society: Washington, DC, 1999.

(35) Kiraly, Z.; Findenegg, G. H. *J. Phys. Chem.* **1998**, *102*, 1203.

electrolyte all reach the same level of saturation surface excess. CTAB has a higher saturation surface excess. These facts indicate the importance of hydrophobic interactions to the adsorbed surfactant morphology. The structures of the adsorbed surfactants have been elucidated. CTAB also has the fastest initial adsorption rate of the surfactants studied, once again due to the greater hydrophobic driving force imparted by the longer hydro-

carbon chain. The adsorption rates for the DTAB, DTAB + 10 mM NaBr, and SDS + 10 mM NaBr systems are quite similar at all concentrations. SDS without added electrolyte has the lowest adsorption rate, due to the electrostatic repulsions between the substrate and the surfactant monomer.

LA026852P